Published online 19 October 2011 *Nucleic Acids Research, 2012, Vol. 40, No. 4* ***1717–1727***
doi:10.1093/nar/gkr855

RecA homology search is promoted by mechanical stress along the scanned duplex DNA

Claudia Danilowicz[1], Efraim Feinstein[1,*], Alyson Conover[1], Vincent W. Coljee[1], Julea Vlassakis[1], Yuen-Ling Chan[2], Douglas K. Bishop[2] and Mara Prentiss[1]

[1]Department of Physics, Harvard University, Cambridge, MA 02138 and [2]Department of Radiation and Cellular Oncology and Department of Molecular Genetics and Cell Biology, University of Chicago, Chicago, IL 60637, USA

Received July 24, 2011; Revised August 30, 2011; Accepted September 26, 2011

ABSTRACT

A RecA–single-stranded DNA (RecA–ssDNA) filament searches a genome for sequence homology by rapidly binding and unbinding double-stranded DNA (dsDNA) until homology is found. We demonstrate that pulling on the opposite termini (3′ and 5′) of one of the two DNA strands in a dsDNA molecule stabilizes the normally unstable binding of that dsDNA to non-homologous RecA–ssDNA filaments, whereas pulling on the two 3′, the two 5′, or all four termini does not. We propose that the 'outgoing' strand in the dsDNA is extended by strong DNA–protein contacts, whereas the 'complementary' strand is extended by the tension on the base pairs that connect the 'complementary' strand to the 'outgoing' strand. The stress resulting from different levels of tension on its constitutive strands causes rapid dsDNA unbinding unless sufficient homology is present.

INTRODUCTION

RecA-family proteins carry out homology search and strand exchange for both programmed homologous recombination and damage-induced recombinational repair (1,2). During RecA-mediated recombination (Figure 1A), protein filaments form on single-stranded DNA (ssDNA) molecules and the resulting nucleoprotein filaments search available double-stranded DNA (dsDNA) molecules for homology (Figure 1A) (1,2). Within a searching ternary complex, ssDNA and dsDNA molecules are bound, respectively, in the stronger and weaker of RecA's two DNA-binding sites—I and II, which run in close parallel along the length of the filament (3–5). During the homology search, short segments of dsDNA are transiently bound in site II (6). Homology search is proposed to involve either base flipping (7) or melting of the dsDNA (8). The RecA bound ssDNA strand, referred to as the 'incoming strand' tests for complementarity with one of the strands of the dsDNA, referred to as the 'complementary strand' (6,9). If sufficient homology is present, the complementary strand of the dsDNA transfers its Watson–Crick pairing from the outgoing strand to the incoming strand, resulting in a heteroduplex dsDNA bound in site I. If homology is not detected, the non-matching dsDNA segment rapidly unbinds. *In vivo*, binding and unbinding must be very rapid to permit genome-wide search for homology on a biologically relevant timescale (10). RecA-family reactions are notable because filament-bound DNA(s) are extended ~1.5× and underwound such that a single helical turn includes ~18 bp rather than the 10-bp characteristic of B-form DNA (11).

The structure of the incoming strand bound in site I consists of nucleotide triplets with nearly B-form structure separated by large rises. The nucleotides are almost perpendicular to the helical axis, as illustrated by the red ssDNA shown in Figure 1B(i) (12). The structure of dsDNA bound in site I is very similar, consisting of nearly B-form base pair triplets separated by large rises. The complementary strand is bound to the filament dominantly through Watson–Crick pairing with the incoming strand (12), as illustrated in Figure 1B(i). The functional role of these triplets has been unclear. The structure of the dsDNA bound in site II and the role that structure plays in homology stringency are also not known. As a result of the work that will be described in this article, we propose that the structure of dsDNA in site II is similar to the structure in site I, but with less mechanical support for the rises, as illustrated by the purple ssDNA strand shown in Figure 1B(i). Consequently, the complementary strand bound to site II is less extended than the

*To whom correspondence should be addressed. Tel: +617 312 0072; Fax: +617 495 0416; Email: feinst@post.harvard.edu

The authors wish it to be known that, in their opinion, the first two authors should be regarded as joint First Authors.

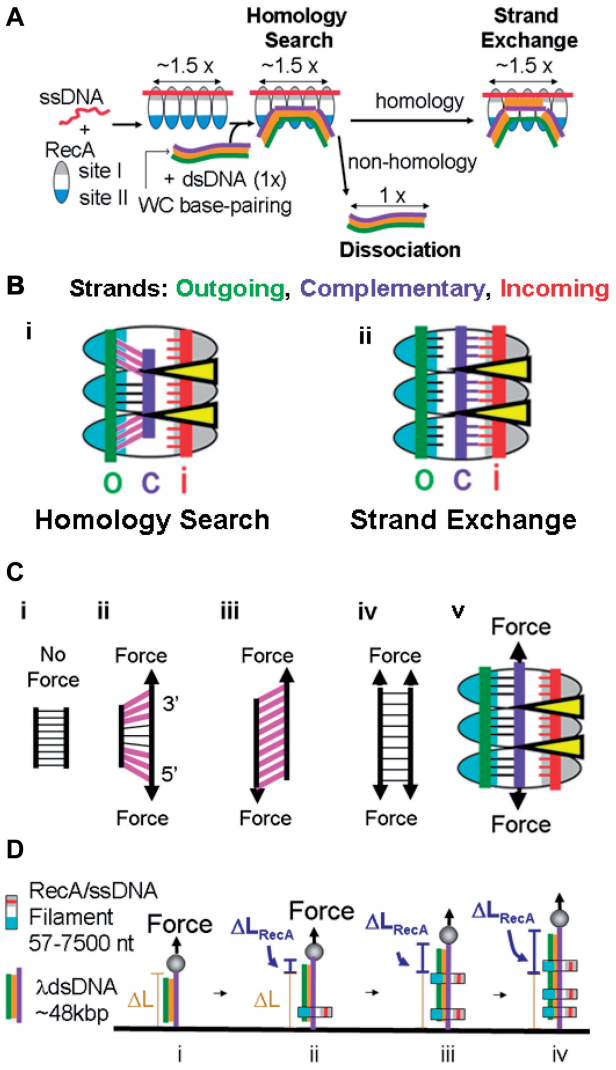

Figure 1. RecA–ssDNA binding to dsDNA. (**A**) Schematic representation of RecA-mediated reactions: incoming ssDNA (red line), outgoing strand (green line), complementary strand (purple line), Watson–Crick pairing (orange) and RecA: site I (gray region of oval) and site II (blue region of oval). (**B**) Schematic representation of the extension and tension on dsDNA bound to RecA–ssDNA filaments with pink highlighting base pairs under tension and yellow triangles indicating regions occupied by the L1 and L2 loops and their attached alpha helices which interact strongly with the incoming strand (i) dsDNA bound to the pre-synaptic filament (ii) dsDNA bound to a RecA–ssDNA filament in the post-strand exchange state (**C**) Schematic representation of the extension and tension on dsDNA with the same color scheme used in (B) (i) in the absence of external force (ii) with external force applied to the 3′5′-ends of one strand (iii) shear force applied to opposite ends of opposite strands (3′3′ or 5′5′ pulling) (iv) with external force applied to both strands at both ends (v) with external force applied to the 3′5′-ends of the complementary strand in the homology searching complex (**D**) Schematic representation of the extension-based assay for measuring the extension of dsDNA due to the binding of RecA–ssDNA filaments (i) λ dsDNA tethered between a capillary tube and a magnetic bead under force (arrow) that is extended without [ΔL, (i)] and with [ΔL_{RecA} (ii–vi)] binding of non-homologous RecA–ssDNA filaments.

complementary strand bound to site I, resulting in a larger lattice mismatch between the complementary and the outgoing strands, as well as a larger tension on the base pairs connecting the complementary and outgoing strands, as illustrated by the pink lines in Figure 1B(i) that indicate base pairs under significant tension. This tension may be released by unbinding when no homology is present or by strand exchange when homology is present [Figure 1B(ii)].

We use experimental measurements of extension of dsDNA due to the binding of dsDNA to RecA–ssDNA filaments as a function of the force applied to the ends of the dsDNA to provide information about the structure of dsDNA bound in site II in the absence of force. The binding of dsDNA to site II in RecA–ssDNA filaments is the first step in the homology recognition/strand exchange process. *In vivo*, if the dsDNA is not homologous, it must rapidly unbind from the RecA–ssDNA filament, but if the dsDNA is homologous, strand exchange should occur quickly. In these experiments, strand exchange cannot occur since the ssDNA molecules in the filaments are non-homologous to the dsDNA. Thus, any observed extension of the non-homologous dsDNA must be the result of the dsDNA binding to the pre-synaptic complex. We apply force to the ends of dsDNA molecules using single molecule magnetic tweezers (13) as represented in Figure 1C and D. Figure 1C(i–iv) illustrates the effect of applying force to naked dsDNA. Figure 1C(i) is a simplified representation of B-form DNA in the absence of force. At the forces considered in this work, the DNA structure is approximately the B-form structure (13–15). However, different pulling techniques produce slightly different variations of the B-form structure, as illustrated in Figure 1C(i–iv). In the interest of clarity, the figures greatly exaggerate the extension difference and the change in extension difference as a function of the distance from the ends of the molecule. Figure 1C(ii) illustrates the effect of pulling on the 3′5′-ends of one strand. Similarly, Figure 1C(iii) shows the effect of pulling on either the 3′3′- or the 5′5′-ends, and Figure 1C(iv) depicts the effect of pulling on both termini. At forces < 60 pN, the measured dsDNA extension does not exceed $1.1\times$ the B-form extension (13–15) (Supplementary Figure S1). Figure 1C(v) illustrates the effect of pulling on the complementary strand when the dsDNA is bound to site II as it is in the pre-synaptic complex, assuming that the extension of the complementary strand of dsDNA bound to site II in the absence of any external force is correctly depicted in Figure 1B(i). Figure 1C(v) shows that pulling on the complementary strand would decrease the extension mismatch between the complementary strand and the outgoing strand, which also reduces the tension on the base pairs connecting the two strands. Such an effect would reduce the free energy cost of the dsDNA extension that normally occurs when the dsDNA binds to site II at zero force (E.F. and M.P., unpublished data). Similarly, it would reduce the free energy decrease that occurs when dsDNA unbinds from site II in the absence of external force. Both of these effects would stabilize the extension of dsDNA bound to site II. Other pulling techniques would not provide as much stabilization as 3′5′-pulling since the other pulling techniques do not compensate as effectively for the stress induced by the protein binding.

We will show that an external force applied to the 3′5′-ends of one strand of a single dsDNA molecule stabilizes the extension of non-homologous dsDNA bound along the entire length of a RecA–ssDNA filament. In contrast, applying the same force to the two 3′, the two 5′, or all four termini does not. Thus, the observed stabilization for 3′5′-pulling is not simply due to a change in the overall dsDNA extension or tension. Rather, it is a result of a differential force on the two dsDNA strands, which probably reduces the extension mismatch and the base pair tension as illustrated in Figure 1C(v). We argue that the specific nature of force-induced stabilization of non-homologous binding reflects a key aspect of the mechanism of the homology search; the differential tension on the two strands of the duplex being searched drives dissociation of the filament in the absence of homology and strand exchange in its presence.

MATERIALS AND METHODS

Applying force along a dsDNA molecule

Experiments were carried out in a square micro-cell (0.8 × 0.8 mm) containing a round inner capillary (0.55 mm in diameter) closed at its ends. The inner capillary was modified by adsorption of 1 mg/ml extravidin in PBS (phosphate buffered saline) pH 7.4 overnight. Double-stranded linear λ genomes (New England Biolabs) were modified by addition of biotinylated oligonucleotides yielding 3′5′-, 3′3′- and 5′5′-dsDNA constructs (Supplementary 'Materials and Methods' section). Samples were prepared by hybridizing and ligating the complementary oligonucleotides. Two, three and four reaction steps were required for the 3′3′-, 3′5′- and 5′5′-samples, respectively. Ligation steps were done in the presence of a thermostable DNA Ligase (Ampligase, Epicentre, Madison, WI). The oligonucleotides at both ends of all these structures included a ssDNA tail [$(dT)_7$-(biotin-$dT)_6$] to allow free rotation of the bonds in the phosphate backbone so no steady state torque can be maintained in the dsDNA molecules. A fourth sample that allows pulling from both termini of both strands was prepared by incubating λ phage dsDNA with biotin-11-dCTP, dATP, dGTP, dTTP and Klenow exo^- polymerase (NEB, Beverly, MA) for 1 h at 37°C, yielding four biotin labels attached to dsDNA. After each modification step was completed, the dsDNA sample was washed three times using Amicon YM-100 filters (Millipore, USA) and 70 mM Tris buffer pH 7.6. The final concentration was determined by the absorbance at 260 nm and the dsDNA sample was diluted to 7 μg/ml before use. These molecules were tethered to capillary walls at one end and to superparamagnetic beads (4.5 μm in diameter, 4×10^8 beads/ml, Invitrogen) at the other end. A 0.2 μl aliquot of each dsDNA at 7 μg/μl in RecA buffer (70 mM Tris–HCl, 10 mM $MgCl_2$ and 5 mM dithiothreitol, pH 7.6) containing 1 mM ATP (or ATPγS) was mixed with free RecA (New England Biolabs) (final concentration 1 μM) or with preparations of RecA–ssDNA filaments (ranging in size from 57 to 7200 nt and final concentration 60 nM) and 1 μl of the beads. DNA filaments were prepared by mixing 3 μM ssDNA (in nucleotides) with 1 μM RecA and 1 mM ATPγS or ATP in 50 μl of RecA buffer. The resulting mixture containing dsDNA, filaments and beads was introduced into the micro-cell. After an initial incubation of 10 min, the DNA molecules became tethered between the glass capillary surface and the extravidin-coated beads. The micro-cell was then placed in our magnetic tweezers apparatus (13) consisting of a stack of permanent magnets whose position relative to the cell can be varied to exert forces between 2 and 200 pN. The position of each bead at constant applied force was followed in real time using an inverted microscope and a digital camera. Each bead was tracked by bead tracking software and recorded using Matlab.

The calibration of the relationship between the force on a magnetic bead and the position of the magnet was originally established using measurements of the Stokes drag on individual magnetic beads in glycerol. This calibration was checked using a Gauss meter to measure the magnetic field as a function of distance from the magnet and using the known magnetization of the magnetic beads to calculate the force. The beads have some variation in magnetization, which means that different beads experience a slightly different force at a given magnet position. The variation in the force is found to be ~5% for these beads. We used the overstretching transition as a standard to calibrate the magnetization for each bead. Earlier work has shown that the overstretching force is 65 ± 1 pN (15), as long as the molecule is not rotationally constrained. The overstretching force for all pulling techniques is the same to within ~1 pN (13,15). Thus, the reported forces are accurate to within 3%.

'Unzipping' DNA molecules with force

Unzipping experiments were performed using the same magnetic tweezers apparatus described above (16). The DNA construct consisted of two λ DNA molecules containing digoxigenin and biotin labels, respectively. The two were ligated to provide one spacer molecule capable of attaching to the capillary and a second dsDNA molecule that can be unzipped by applying force to the magnetic bead attached to its free end. In these experiments Dynal 2.8 μm beads coated with Streptavidin were used and capillaries were coated with antidigoxigenin IgG. Samples containing RecA buffer, 1 μl of the unzipping construct, 1 μl of the beads, 1 μl of RecA-M13ssDNA filaments 60 nM (in nt) final concentration (or 1 μM of free RecA) and 1 mM ATPγS were incubated in the micro-cell. The unzipping curves were obtained by increasing and decreasing the force at a rate of ~1 pN/s between 1 and 20 pN. During these cycles the position of each bead was followed as described above.

Single molecule fluorescence microscopy

RecA protein was labeled with Alexa Fluor 568 dye (Invitrogen) using conditions recommended by the supplier. A 50-μl aliquot of 2 mg/ml RecA was dialyzed overnight in PBS pH 7.4. A 1-μl aliquot of the provided solid dye dissolved in 500 μl of 100 mM sodium bicarbonate

solution was added to the dialyzed RecA and incubated for 1 h at room temperature. The modified protein was purified from unbound dye by ultrafiltration in PBS using Amicon YM-10 filters. We have shown that the labeling procedure does not reduce the activity of the protein using a conventional ensemble D-loop assay (Supplementary Figure S2).

The filaments obtained with labeled RecA were prepared and used as described above. Fluorescence images were obtained on an Olympus FV300 microscope with a Perkin-Elmer spinning disk and imaged on a Hammamatsu EMCCD camera, with laser excitation at 561 nm. Force was applied by controlling the distance between a small permanent magnet and the capillary during the fluorescence measurement.

Data analysis

Data analysis was performed using scripts custom-written in Matlab (www.mathworks.com). We developed an automated algorithm to detect intervals of paused filament growth from growth curves (bead position versus time) as follows: direct examination suggested that growth does not occur at a constant rate over the observation period, but instead can be modeled as a sequence of intervals with constant growth rate, separated by abrupt stochastic changes in growth rate. To identify intervals of constant growth, we choose an initial starting point at time $t = 0$. Then we performed linear least-squares fits on all subintervals of the growth curve beginning at the starting point and lasting at least 2 s. We chose as 'best fit' the line with the minimum absolute value of the sum of its residuals per unit length multiplied by the sum of the auto-correlation of its residuals. Then we set the endpoint of this best fit line as the starting point to seek a new best fit, proceeding iteratively until the entire growth curve was exhausted. We allowed the algorithm to skip short regions (<1 s) of high noise at the transitions between intervals with different growth rates. Because the exact positions of transitions between intervals with different growth rates are uncertain, we allowed a 0.5-s overlap between successive intervals. We considered pauses to be intervals beginning >10 s after a change in force, during which the best fit growth rate was <0.15 nm/s.

RESULTS

Tension stabilizes non-homologous interaction between dsDNA and RecA–ssDNA filaments

The ends of non-homologous 50 kb λ dsDNA molecules were pulled by magnetic tweezers in the presence of RecA–ssDNA filaments (Figure 1D). These RecA–ssDNA filaments were formed on bacteriophage M13mp18 circular ssDNA ~7200 nt. Binding was examined by confocal microscopy using fluorescently labeled RecA (Figure 2). The labeled RecA protein was shown to be fully functional using a conventional D-loop assay (Supplementary Materials and Supplementary Figure S2). At ~55 pN of applied force, one or two bright fluorescent foci are reproducibly seen as ovals elongated along the trajectory between the slide and a magnetic bead. The position of the foci differed from one binding event to the next; once bound, the position of the foci on the DNA did not change until unbinding occurred in response to a reduction of force <50 pN. If the magnet position is fixed, foci do not move over ~10 min. If the magnet is moved back and forth, the bead-bound end of the tethered DNA and the foci move coordinately in response. Thus, the presence of external force, along one strand of a dsDNA, permits stable binding of RecA–ssDNA filaments in the absence of homology. No binding occurs at forces <50 pN consistent with zero-force solution studies (17–19).

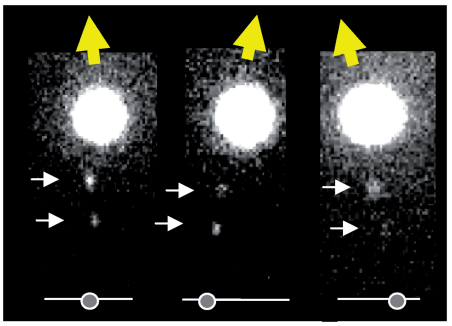

Figure 2. RecA–ssDNA filaments bind to non-homologous dsDNA pulled by 3′5′ ends. Confocal microscope visualization (linearly enhanced for brightness and contrast) of fluorescent RecA–ssDNA filaments (white arrows) bound to λ dsDNA. The force applied to the bead is indicated by the yellow arrows.

Quantitative force/extension analysis involving unlabeled non-homologous RecA–ssDNA filaments confirm and extend this conclusion. Here, dsDNA lengths were measured with ~10 nm accuracy, at 0.2 s intervals, during time periods when the applied force was constant. When the dsDNA is subjected to 3′5′-pulling, the bead-to-capillary distance corresponding to the dsDNA length increases beyond that seen without RecA, indicating ternary complex formation (ΔL_{RecA}, Figure 1D). Binding signals were measured for >1000 single molecules for filaments on linear ssDNAs of 57–7200 nt. Binding is observed at forces >50 pN (Figure 3A, blue dots). A critical feature of our approach is that, in the absence of added RecA–ssDNA filaments, forces of <62 pN result in little change in the length of DNA relative to B-DNA (Figure 3A, red dots; Supplementary Text and Supplementary Figure S1).

Representative single molecule binding profiles for a 1000-nt filament (Figure 3B) illustrate successive binding plateaus at appropriately quantized lengths (dashed lines, 1–4). For these curves, the filaments were prepared in a buffer containing ATPγS, but the measurements were made in a buffer containing ATP. Plateaus are linked by progressive length extensions, with some pausing at intermediate lengths (Figure 3B). ΔL_{RecA} increases by ~170 nm between each plateau, i.e. 1000 bp of dsDNA bound and extended to ~0.51 nm/bp (Figure 3B), or 1.5× the canonical B-DNA extension of 0.34 nm/bp (20). This total extension/bp corresponds to a ΔL_{RecA} of ~0.17 nm/nt. Similar plateaus are seen by detailed analysis of all single molecule extension versus time curves in a buffer containing ATP.

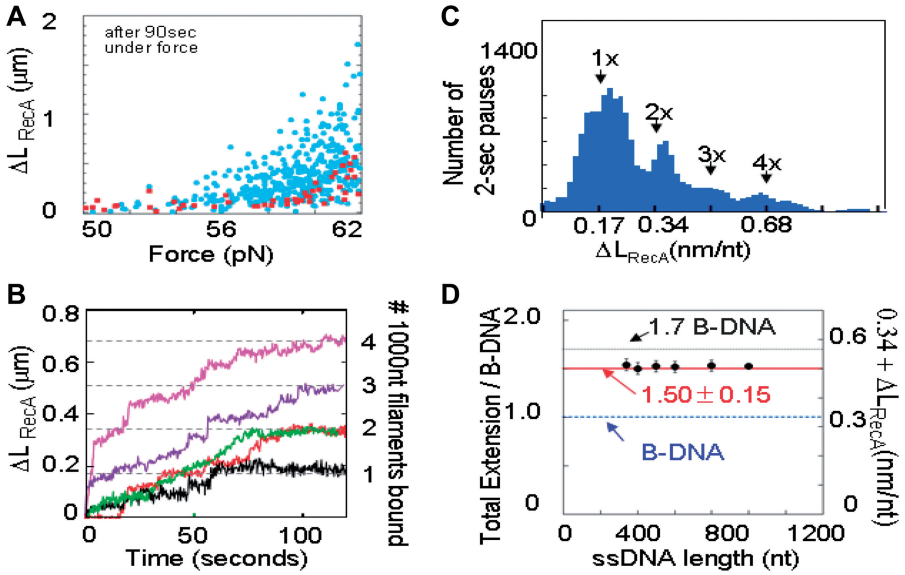

Figure 3. RecA–ssDNA filaments extend non-homologous dsDNA pulled by 3′5′ ends. (**A**) ΔL_{RecA}'s for λ dsDNAs controls with free ssDNA or λ dsDNA only (red, $N = 87$) and λ dsDNAs with RecA–ssDNA filaments (blue, $N = 454$). (**B**) Single molecule extension profiles for non-homologous binding. Different colors are used to represent the response for each different single molecule. The curves ending at positions corresponding to 1, 3 and 4 filaments are 57.0, 59.0 and 60.9 pN, respectively. The red and green curves ending at two-filament lengths correspond to 58.9 and 57.2 pN, respectively. The filaments were prepared in a buffer containing ATPγS, but measured in a buffer containing ATP Pauses at full filament lengths are indicated by horizontal bars the same color as the curve. (**C**) ΔL_{RecA} probability distributions for periods of ≥2 s constant λ dsDNA length, for all filaments of 400–800 nt at 50–62 pN. (**D**) DNA extensions within homology search complexes on dsDNA (color) or λ ssDNA.

To quantify the extensions that characterize these plateaus, each single molecule extension versus time curve was examined for intervals of ≥2 s wherein the dsDNA length was effectively constant ($\Delta L_{RecA}/\Delta t \leq 0.15$ nm/s). Correspondingly, compilation of data for filaments of many ssDNA lengths, at forces ≤62 pN, reveals a series of peaks corresponding to full-length binding of integer numbers of filaments with an extension of 0.51 ± 0.03 nm/bp (Figure 3C and D and Supplementary Figure S3). 3′5′-pulling stabilizes non-homologous binding regardless of which strand of λ dsDNA is pulled, and full length extension has been observed for more than 10 different sequences with lengths from 150 to ~7200 nt. Thus, the extension of dsDNA along non-homologous RecA–ssDNA filaments is independent of base composition or sequence.

In contrast to the results obtained with pulling on 3′5′ on the same component single strand, no significant extension occurs under identical reactions. λ dsDNA is pulled from its two 3′-strand termini, from its two 5′-strand termini, or from both termini of both strands. In these cases, the dsDNA length increase seen in the presence of RecA–ssDNA filaments did not exceed that for dsDNA alone (Figure 4). Figure 4A shows plots of ΔL_{RecA} as a function of force, after the force has been applied for 60 s. The experimental curves are shown in magenta and the results for the controls are shown in dark gray. Each point corresponds to one single measurement made on a single molecule. The ssDNA used in the filaments is a 1000-nt subregion of pcDNA3. Figure 4B and C shows histograms of ΔL_{RecA} measured after a force has been applied for 60 s for force ranges from 52 to 55 pN and 52 to 57 pN. For comparison, the overstretching transition occurs at 65 pN and is approximately 1 pN wide. Figure 4D shows a summary of the data in Figure 4B and C for both force ranges.

The results in Figure 4 clearly indicate that when the dsDNA is pulled from the 3′5′-ends, ΔL_{RecA} measured in the presence of free ssDNA–RecA filaments significantly exceeds the ΔL_{RecA} measured in the absence of filaments. In contrast, none of the results for the other pulling techniques result in DNA extension that significantly exceeds the amount of extension observed in the controls. We note that at forces <80 pN the extension versus force curves for naked dsDNA are similar for all pulling techniques (13,14). In particular, the overstretching forces for all pulling techniques are the same to within ~1 pN (13,14).

For all of the results shown in Figure 3, we pulled the 3′5′-ends of one of the constituent strands, but similar results were obtained when we pulled on the 3′5′-ends of the other constituent strand as can be seen in Figure 5. Note that the data shown in Figure 5 was obtained after filaments were prepared in a buffer containing ATPγS, and the measurements were made in a buffer containing ATPγS, whereas the results shown in Figure 3 correspond to filaments prepared in ATPγS and measured in ATP. We also did experiments where the filaments were prepared in ATP and measured in ATP. We performed measurements in all three buffers to make sure that we did not see any artifacts associated with the instability of the binding of the RecA to ssDNA in the RecA–ssDNA filaments. We found similar results for all three buffer conditions, but the extension observed in ATPγS occurs at a

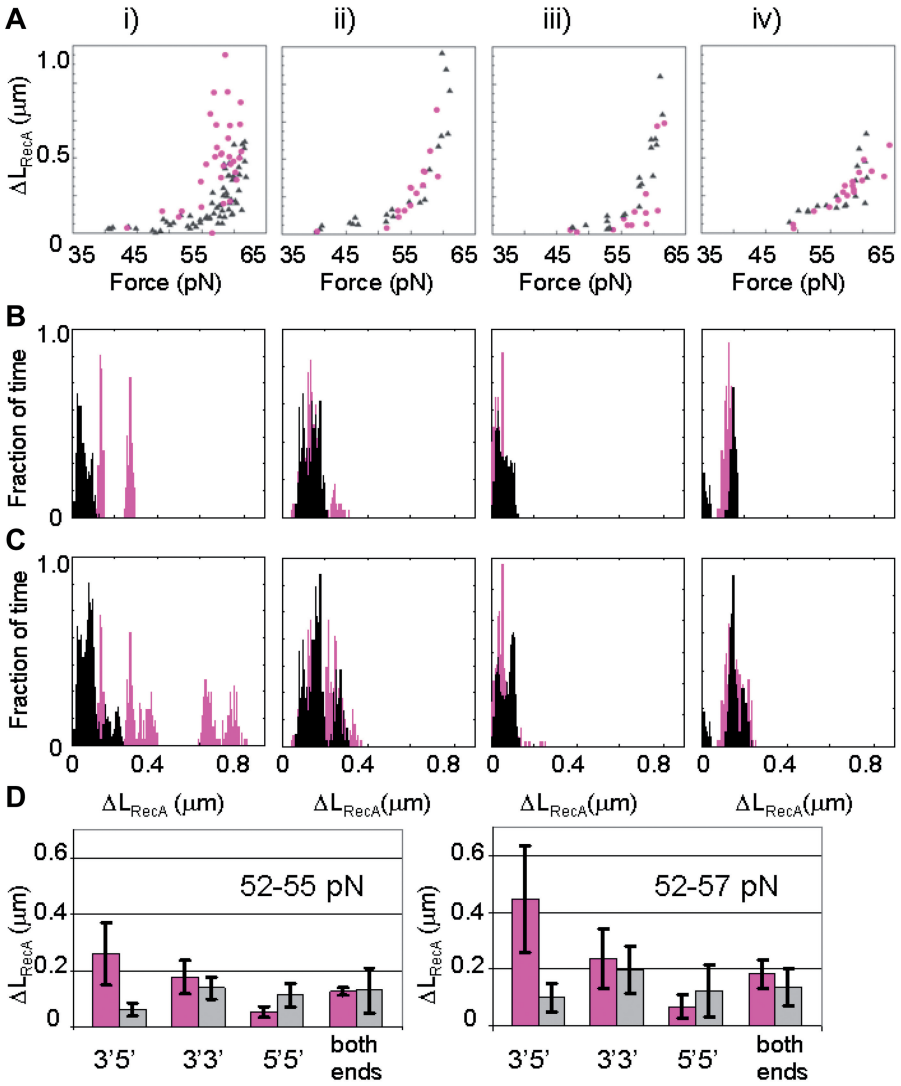

Figure 4. Binding of RecA–ssDNA filaments to dsDNA pulled from different ends. (**A**) ΔL_{RecA} versus force for 1000-nt filaments (magenta circles). λ dsDNAs are pulled on (i) 3′5′-ends of one strand, (ii) 3′3′-ends, (iii) 5′5′-ends, (iv) both ends of each of the two constituent strands of the dsDNA, respectively, and controls for each pulling technique in the absence of RecA (gray triangles). (**B**) Histograms of the fraction of the total number of beads that showed a particular ΔL_{RecA} after a force has been applied for 60 s (magenta) for dsDNA pulled (from left to right) from 3′5′-ends of one strand, 3′3′ends, 5′5′-ends, and both ends of each of the two constituent strands of the dsDNA; force range: 52-55 pN and negative controls shown in gray. (**C**) Histograms of the fraction of the total number of beads that showed a particular ΔL_{RecA} after a force has been applied for 60 s (magenta) for dsDNA pulled (from left to right) from 3′5′-ends of one strand, 3′3′-ends, 5′5′-ends and both ends of each of the two constituent strands of the dsDNA: force range: 52–57 pN; negative controls shown in gray. (**D**) Bar graphs for ΔL_{RecA} values between 52 and 55 pN and 52 and 57 pN, for 1000-nt filaments. λ dsDNAs are pulled 3′5′-, 3′3′-, 5′5′- and both ends of both strands: positives (magenta) and controls (gray). In these experiments filaments were prepared in a buffer containing ATPγS and measured in a buffer containing ATPγS.

slightly lower force than the corresponding extensions observed in ATP. In addition, the extension increases are more abrupt and the pauses during or between individual assimilation events are more marked when extensions are performed in the presence of ATP as shown in Figure 3B, than they are in the presence of ATPγS, as shown in Figure 5. We have yet to fully characterize the mechanism underlying this difference, but it may be due to a dependence of the affinity on the nature of the bound nucleotide cofactor. We note that such a difference is known to exist for dsDNA binding to site I in RecA (21–23).

Tethered dsDNA is not constrained from rotation

In the magnetic tweezers apparatus, the magnetic bead should be free to rotate because the magnetic field direction is parallel to the direction of the dsDNA. Of course there will always be some small component of the magnetic field that is perpendicular to the direction of the dsDNA, and it is possible that a small residual field might rotationally constrain the bead. To probe this possibility, we exploited the known result that if the dsDNA is rotationally constrained then at applied forces between 3.6 and 10 pN, <15% of the dsDNA is covered by RecA (24). The stalling of the RecA growth was attributed to the torque

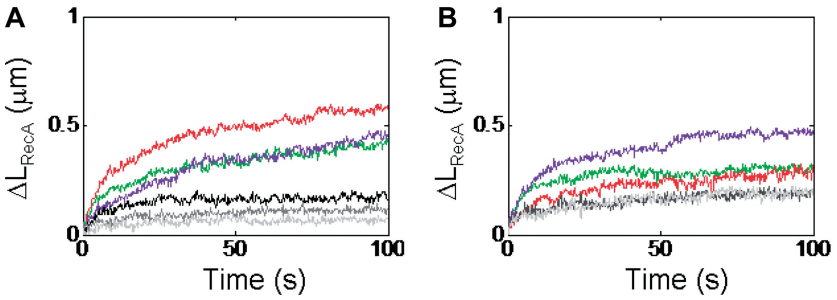

Figure 5. Single molecule extension profiles for non-homologous RecA–ssDNA (1 kb) filaments binding when force is applied to the 3′5′-ends of one of the constituent strands in RecA buffer pH 7.6 containing ATPγS. (**A**) Force applied to the same constituent strand as in Figure 3. Green curve: 55.7 pN, red: 59.1 pN, and purple: 58.4 pN. Control curves are black (56.6 pN), dark gray (59.8 pN) and light gray (57.5 pN). (**B**) Force was applied to the 3′5′-ends of the other constituent strand. Green: 56 pN, red: 59.6 pN, and purple: 58.4 pN. Control curves are light gray (59 pN) and dark gray (57.5 pN).

on the dsDNA that occurs because RecA polymerization underwinds the dsDNA and the resulting torque cannot be relaxed if the dsDNA is rotationally constrained. This result is consistent with earlier solution measurements that show that the torque build up due to RecA polymerization limits the extent of additional RecA polymerization on dsDNA (11). In sharp contrast with the result for rotationally constrained dsDNA, we observe that when a 9 pN force is applied to dsDNA that is tethered by all four termini the extension increase significantly exceeds 15% (Supplementary Figure S4).

When the dsDNA is bound between the magnetic bead and the surface by ssDNA tails, as it is for 3′5-′, 3′3′- and 5′5′-pulling, the ssDNA tails allow free rotation of the dsDNA. If the DNA were non-specifically bound or the ssDNA tails were linked to the surface by RecA in a manner that did not allow free rotation, then we should not observe any difference associated with different pulling techniques. Figure 4 shows significant differences between the experimental results for dsDNA pulled from the 3′5-′, 3′3′- and 5′5′-ends interacting with RecA–ssDNA filaments. Thus, most of the dsDNA molecules must be correctly tethered by their ssDNA tails rather than being non-specifically bound in a way that would disallow free rotation. The experimental results presented above suggest that for 3′3-′, 5′5-′, 3′5′-pulling and pulling from both termini of both strands, the dsDNA is not rotationally constrained. Thus, no global torque can be maintained, so the dsDNA cannot be globally underwound or overwound.

Together, all of the results discussed above suggest that the observed extension increases that result when dsDNA is pulled from the 3′5′-ends are not simply a consequence of the tension on the dsDNA or of the resulting extension. They are also not the result of a global torque or of pulling on a particular strand of the dsDNA. Thus, the results suggest that the observed stable binding of non-homologous RecA–ssDNA filaments to dsDNA is a consequence of a structural change in the dsDNA that occurs only when a force is applied to both ends of one single dsDNA strand.

Non-homologous interactions of dsDNA under tension with RecA–ssDNA filaments are less stable than interactions with free RecA

If binding is established by 3′5′-pulling as noted above, and force is then reduced or eliminated, bound filaments rapidly unbind (Figure 6A–D). Maintenance of binding requires continued imposition of >50 pN of force, regardless of whether ATP hydrolysis is occurring, since force is required to maintain binding in buffers containing either ATP or ATPγS. Thus, unbinding of non-homologous RecA–ssDNA filaments from dsDNA does not require hydrolysis, consistent with previous zero force results that showed homology search and strand exchange can occur in ATPγS (19).

In contrast to the above results for binding of dsDNA in site II of a RecA–ssDNA filament, it is well known that the binding of the dsDNA to RecA in the post-strand exchange product is stable even in the absence of force until ATP hydrolysis occurs (25), though rapid unbinding occurs in the presence of hydrolysis (26). Since dsDNA in the post-strand exchange complex is bound in site I of RecA, properties of this complex are often probed via measurements of direct binding of RecA to dsDNA, which occurs via site I (26–29). In our system, in accord with previous studies, such binding results in an extension/bp of 0.52 ± 0.03 nm/bp (Supplementary Figure S1) and no force is required to maintain site I binding in the absence of hydrolysis (Figure 6F and H). Interestingly, however, unbinding of RecA in the presence of ATP hydrolysis is blocked by imposition of external tension, with all modes of pulling being equally effective (Figure 6E and Supplementary Figure S5). This result is consistent with similar results from a previous study of dsDNA binding to site I in the eukaryotic RecA homolog Rad51 (30). The results argue that the non-homologous interactions of dsDNA with RecA–ssDNA filaments described above do not involve binding of free RecA to dsDNA via site I following dissociation of RecA from ssDNA.

Zipping and unzipping DNA experiments show that non-homologous interactions of RecA–ssDNA filaments with ssDNA under tension are more stable than those with dsDNA under tension

Additional experiments were carried out to demonstrate that the full-length non-homologous strand assimilation observed is from interaction with dsDNA and not a constituent ssDNA strand created by force-induced melting. The experiments used a different tethering scheme than that used for dsDNA pulling experiments. This scheme applies a mechanical force directly to each of the two

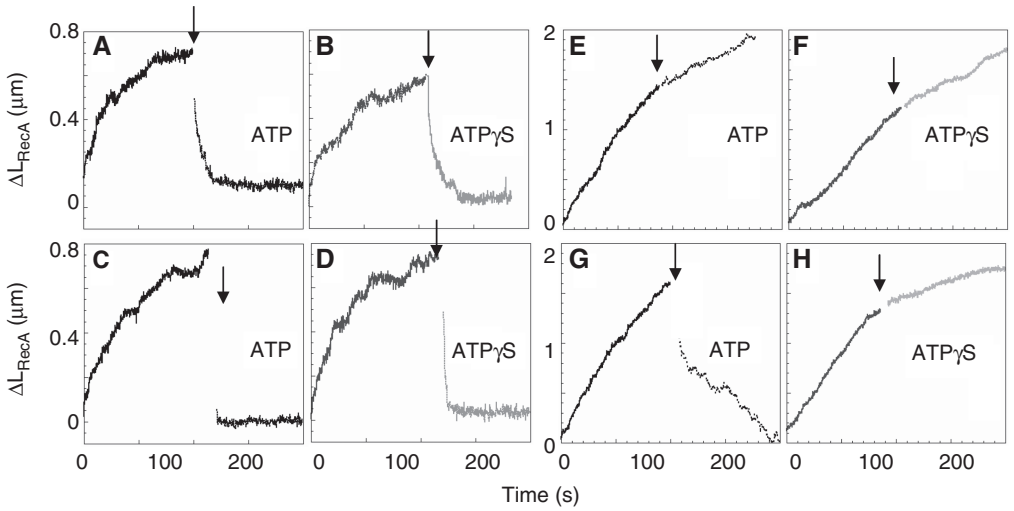

Figure 6. Non-homologous binding is stabilized by external force. Preformed RecA–ssDNA filaments (**A–D**) or free RecA (**E–H**) added to λ dsDNAs. After 100 s at 57 pN, force was reduced (arrow) by 10 to 47 pN (**A, B, E, F**) or 40 to 17 pN (**C, D, G, H**). Non-homologous RecA–ssDNA binding is rapidly lost if force is reduced, irrespective of ATP hydrolysis (**A, D**). RecA binding (via site I) continues in ATPγS (**F, H**) and is lost in ATP if force is reduced <30 pN (**E, G**).

strands at one terminus of the double helix (31). In this scheme, two double-stranded λ genomes are connected by intermolecular ligation of one ssDNA strand. One of the two duplex λ genomes is tethered to the capillary and serves as a spacer to separate the bead from the capillary wall (λ_{sp}). The second λ genome (λ_{μ}) carries the magnetic bead on its unligated end at the junction between the two phage genomes. On the end of λ_{μ} opposite to the ligation junction, a DNA hairpin connects its component ssDNA strands (Figure 7A). This configuration makes it possible to fully denature λ_{μ} by exerting force on the bead, a process we refer to as 'unzipping' (Figure 7B). The distance between the magnetic bead and the capillary surface increases with increasing force as the dsDNA is converted to ssDNA (Figure 7B). At ~18 pN, λ_{μ} is fully unzipped, though λ_{sp} remains completely double stranded. Once the λ_{μ} is fully unzipped, the separation between the bead and the capillary increases only slightly with further increases of force as a result of extension of λ_{μ} ssDNA and λ_{sp} dsDNA. Starting with fully unzipped λ_{μ}, reduction of force to <~10 pN results in a major length transition as ssDNA re-zips [Figure 7C and descending curve (a) in Figure 7D]. The extension versus force curves for increasing and decreasing force are different. This hysteresis is a result of the difference between the force required to unzip GC sequences and the force required to rezip AT sequences (32). When the λ_{μ} is fully rezipped, the separation between the bead and the capillary is again equal to the length of λ_{sp}. This cycle of unzipping and rezipping can be repeated many times, and the curves are reproducible.

Thus, it is possible to determine the effect of a non-homologous RecA–ssDNA filament binding to ssDNA by monitoring the extension versus force curves for repeated cycles of unzipping and rezipping. If the RecA–ssDNA filaments bind to the ssDNA tightly enough that they block Watson–Crick pairing, then the measured extension in the presence of the bound filaments will be longer than the extension in the absence of the filaments because rezipping will be blocked. In order to distinguish the components of the extension versus force curve contributed by rezipping from those contributed by any additional extension/contraction of the ssDNA or the λ_{sp} duplex, a control curve was constructed by adding the values from extension versus force curves obtained with λ_{sp} alone with two times those obtained from a curve generated with ssDNA obtained from thermal melting of λ dsDNA [Figure 7D, curve (b)]. This ssDNA cannot rezip because of the absence of the complementary strand. The difference between the 'unrezippable' control curve and the curve obtained with the tethered λsp–λμ alone is taken to reflect DNA rezipping.

Using this system, the interaction of RecA-M13 ssDNA filaments with ssDNA under tension was determined by adding RecA-M13 ssDNA filaments to the reaction chamber, and then unzipping tethered DNA to establish a starting point. Force was then reduced and an extension versus force curve recorded. Comparison of the extension versus force curves generated in this way to the curve generated in the absence of added nucleoprotein filament and the 'unrezippable' control showed that the RecA–ssDNA filaments block re-zipping almost completely [note the similarity of curve (c) to curve (b) in Figure 7D]. Re-zipping of the naked ssDNA was complete at forces <8 pN, but reactions containing RecA–ssDNA filaments remained largely unzipped even at forces <5 pN. Importantly, the interaction of RecA–ssDNA to unzipped ssDNA at forces <5 pN contrasts with the interaction of RecA–ssDNA to dsDNA described above, which is lost at forces <50 pN. Once the DNA had been allowed to rezip, force was increased a second time to generate an unzipping extension versus force curve. This experiment confirmed that little or no rezipping had occurred in the experiments with RecA-M13ssDNA. The ascending curve again showed strong similarity to the unrezippable control. These results indicate that non-homologous binding of

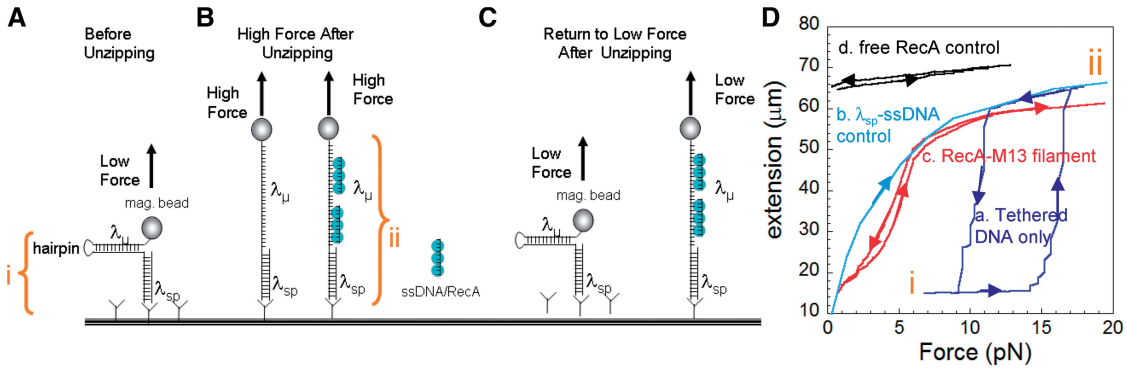

Figure 7. Interaction of RecA–ssDNA filaments with ssDNA during DNA 'unzipping'. Representation of unzipping experiment: One λ dsDNA molecule (λ_{sp}) acts as spacer and the second λ dsDNA (λ_{μ}) is unzipped by force. λ_{μ} contains a hairpin connecting its two constituent ssDNA strands at one terminus and a magnetic bead at the free terminus between λ_{sp} and λμ. i is the extension distance for forces between ~ 2 and 12 pN at which λ_{sp} B-form duplex molecule is stretched out, but the λ_{μ} molecule remains fully zipped. ii is the extension distance at which λ_{μ} is fully unzipped, but the λ_{sp} remains in B-form. (**A**) The initial extension before unzipping. (**B**) The extension after unzipping while a force >15 pN is maintained. (**C**) The extension after the force has been lowered to ~5 pN. (**D**) Extension versus force curves for unzipping. The force was first increased and then decreased. (**a**) No added protein or nucleoprotein filaments (**b**) 'unrezippable' control curve constructed by taking the sum of the extension versus force curves for λ_{sp} alone and two times that for a λ ssDNA strand obtained by thermal melting of dsDNA. (Note: in this case rezipping is impossible because the complementary strand is not present.) (**c**) Unzipping in the presence of RecA–ssDNA filaments (M13 ssDNA). (**d**) Unzipping in the presence of free RecA protein. In (a), (c) and (d) curves generated by increasing force differed from those generated by decreasing force. In these cases, upturned arrowheads mark the ascending curves and down-turned arrowheads the descending ones.

RecA–ssDNA to ssDNA under tension is sufficiently stable so as to prevent 'rezipping' at forces far below those required to stabilize RecA–ssDNA binding to dsDNA even in the presence of competition with the Watson–Crick pairing with sequence matched ssDNA.

Substitution of RecA–ssDNA filaments with free RecA provided a control to confirm that the interactions observed with filaments resulted from interaction of site II with the unzipped ssDNA rather than site I. Reduction of force did not result in rezipping at saturating levels of free RecA [Figure 7D, curve (d)]. The filaments formed with free RecA are also longer and stiffer than unzipped ssDNA in the absence of RecA. Taken together, the unzipping experiments provide strong evidence that tension-dependent non-homologous interaction of RecA–ssDNA with tethered dsDNA involves assimilation of both strands of the duplex and not a single component ssDNA strand.

Addition of excess ssDNA blocks interaction of RecA–ssDNA filaments with dsDNA under tension

Finally, additional experiments were performed in the presence of an excess of ssDNA that is free to bind to site II in the RecA–ssDNA filaments. Earlier work has shown that such an excess can block interactions between RecA–ssDNA filaments and free dsDNA in the absence of external force (33). We found that the free RecA–ssDNA also blocked the interaction in the presence of a force on the dsDNA, providing another independent line of evidence indicating that the extension we observe depends on the binding of the dsDNA to site II in the RecA–ssDNA filament.

DISCUSSION

We show that RecA–ssDNA–dsDNA complexes corresponding to those that arise during homology search *in vivo* are stabilized by pulling along either strand of the dsDNA (3′5′-pulling), and not by other pulling modes. These experimental results exclude some possible explanations of the force-induced stabilization of binding of dsDNA to RecA–ssDNA filaments. For example, the observed force-induced stabilization cannot be explained by any model based simply upon DNA extension or tension (27,34) because, in such cases, all four pulling modes should have been similarly effective. In contrast, tension- or extension-based explanations may explain the stabilization of dsDNA binding to site I in RecA since all pulling techniques stabilize that binding. Similarly, explanations based on a reduction of the compression on the RecA are excluded because pulling on both termini of both strands does not stabilize the binding. Thus, for effects of pulling on the RecA–ssDNA–dsDNA complex, we only consider explanations that depend on structural changes that result from pulling on both ends of either one of the two constituent strands of the dsDNA.

The structure of dsDNA bound to site II is not available, but some properties of the structure may be inferred from experimental results in this article and other structural and functional information. Our experimental results show that the average extension/bp for the force-dependent ternary filament (Figure 3D) is ~0.51 nm/bp, which is also the same as the average extension/bp of both ssDNA (Figure 7D) and DNA in site I (Supplementary Figure S1). Therefore, strand exchange and its concomitant breaking and formation of hydrogen bonds do not alter the average extension/bp of the bound dsDNA, consistent with earlier work (6). Similarly, earlier functional studies of the pre-strand exchange complex suggested that the complementary strand explores Watson–Crick pairing interactions with the incoming strand site via base flipping (3,7). Theoretical work has shown that such base flipping occurs readily if the bases are perpendicular to the DNA

axis (35,36), as they are when either dsDNA or ssDNA is bound to site I (12). If strand exchange simply occurs through flipping of bases that are nearly perpendicular to the helical axis, then the functional and theoretical studies suggest that the structure of dsDNA bound to site II must include the following features: (j) the complementary strand must be bound dominantly through Watson–Crick interactions with the outgoing strand (3,12), (ii) bases in the outgoing strand bound to site II must be approximately perpendicular to the helical axis and have a triplet structure with large rises that is in registration with the triplet structure in the incoming strand. Thus, functional studies and studies of the average extension/bp both suggest that the structure of dsDNA bound to site II is very similar to the structure of dsDNA bound to site I.

We propose that the triplet structure of dsDNA bound to site II with the complementary strand bound dominantly through base-pair interactions to the outgoing strand results in stress on the base pairs connecting the outgoing and complementary strands (Figure 1B). In the absence of 3′5′ pulling or strand exchange, this free-energetically unfavorable stress due to the rises between the base pair triplets causes rapid dissociation of dsDNA. Correspondingly, stabilization of site II binding by 3′5′ pulling results from reducing the stress on the base pairs [Figure 1C (v)]. We propose that we are relieving the stress by pulling on the complementary strand. However, we cannot completely exclude the possibility that we are relieving stress by pulling on the outgoing strand.

Though the experimental results presented in this article considered the binding of RecA–ssDNA filaments to non-homologous dsDNA, we believe that the results have implications for the sequence dependence of the stability of the post-strand exchange product. It is well known that if strand exchange occurs, the dsDNA binding to the post-strand exchange complex is stable at zero force despite the dsDNA extension [until ATP hydrolysis occurs; refs (26,27)] [Figure 1C(v)]. The same is true for RecA filaments formed by direct binding of RecA to dsDNA via site I (Figure 6E–H). In the post-strand exchange product, the free energy increase associated with the rises between the triplets in the dsDNA bound in site I must be overcome by the free energy decrease due to contacts between the dsDNA and site I amino acid residues (12), whereas for dsDNA bound in site II we propose that the triplet rises make the dsDNA binding free energetically unfavorable. Thus, transferring the triplet rises from site II to site I would stabilize the binding of dsDNA to the RecA filament. In contrast, failure to make such a transfer would leave the dsDNA bound to the filament in a state that is free energetically unfavorable, promoting rapid unbinding of the dsDNA. Given that strand exchange within a triplet is free energetically unfavorable unless homology is perfect, this model then suggests that strand exchange could not be stable unless at least six bases of contiguous homology are present.

Though the transfer of 6 bases is the minimum length that could possibly be stable, the proposed model suggests that the transfer of more rises would result in a more stable strand exchange product until the probability that the strand exchange product will spontaneously unbind due to thermal fluctuations becomes negligible because the binding is so free energetically favorable. This suggestion is consistent with the experimental results that show that although the strand exchange product due to 8 nt is sufficiently stable to be observable, the stability of the post-strand exchange product increases with sequence length until an asymptotic value is achieved when ~18 contiguous nucleotides are homologous (9).

Given that short (~9 bp) regions of accidental contiguous homology are very common in the genome, the formation of stable strand exchange products in such regions of accidental homology would preclude homology searching from occurring on a biologically relevant timescale. We propose a model in which dsDNA bound to the pre-synaptic complex receives less mechanical support than the dsDNA in the post-strand exchange product. This model predicts that stable strand exchange would require at least ~12 nt of contiguous homology, but the stability of the strand exchange product of longer sequences would become insensitive to heterology as long as the sequence included ~12 nt of contiguous homology.

SUPPLEMENTARY DATA

Supplementary Data are available at NAR Online: Supplementary Material and Methods, Supplementary Text, Supplementary Figures 1–5, Supplementary References [9,12–14].

ACKNOWLEDGEMENTS

The authors thank Jeffrey Carey and Jennifer Grubb for the preparation of selected DNA substrates and Nancy Kleckner for useful discussions and suggested revisions. Some work for this article was performed at the microscopy facilities of the Harvard Center for Biological Imaging.

FUNDING

This work and C.D. were supported by grants from the National Institutes of Health (GM025326, GM050936 to D.K.B.), Harvard University (to M.P.). Funding for open access charge: Harvard University.

Conflict of interest statement. None declared.

REFERENCES

1. Kowalczykowski,S.C. and Eggleston,A.K. (1994) Homologous pairing and DNA strand-exchange. *Annu. Rev. Biochem.*, **63**, 991–1043.
2. Roca,A.I. and Cox,M.M. (1990) The RecA protein: structure and function. *Crit. Rev. Biochem. Mol. Biol.*, **25**, 415–456.
3. Howard-Flanders,P., West,S.C. and Stasiak,A. (1984) Role of RecA protein spiral filaments in genetic recombination. *Nature*, **309**, 17–23.
4. Müller,B., Koller,T. and Stasiak,A. (1990) Characterization of the DNA binding activity of stable RecA-DNA complexes.

Interaction between the two DNA binding sites within RecA helical filaments. *J. Mol. Biol.*, **212**, 97–112.
5. Takahashi,M., Kubista,M. and Nordén,B. (1989) Binding stoichiometry and structure of RecA-DNA complexes studied by flow linear dichroism and fluorescence spectroscopy. Evidence for multiple heterogeneous DNA co-ordination. *J. Mol. Biol.*, **205**, 137–147.
6. Xiao,J., Lee,A.M. and Singleton,S.F. (2006) Direct evaluation of a kinetic Model for RecA-mediated DNA-strand exchange: The importance of nucleic acid dynamics and entropy during homologous genetic recombination. *ChemBioChem*, **7**, 1265–1278.
7. Folta-Stogniew,E., O'Malley,S., Gupta,R.C., Anderson,K.S. and Radding,C.M. (2004) Exchange of DNA base pairs that coincides with recognition of homology promoted by E. coli RecA protein. *Mol. Cell*, **15**, 965–975.
8. Adzuma,K. (1992) Stable synapsis of homologous DNA molecules mediated by the Escherichia coli RecA protein involves local exchange of DNA strands. *Genes Dev.*, **6**, 1679–1694.
9. Hsieh,P., Camerini-Otero,C.S. and Camerini-Otero,R.D. (1992) The synapsis event in the homologous pairing of DNAs: RecA recognizes and pairs less than one helical repeat of DNA. *Proc. Natl Acad. Sci. USA*, **89**, 6492–6496.
10. Camerini-Otero,R.D. and Hsieh,P. (1993) Parallel DNA triplexes, homologous recombination, and other homology-dependent DNA interactions. *Cell*, **73**, 217–223.
11. Stasiak,A., Di Capua,E. and Koller,T. (1981) Elongation of duplex DNA by recA protein. *J. Mol. Biol.*, **151**, 557–564.
12. Chen,Z., Yang,H. and Pavletich,N.P. (2008) Mechanism of homologous recombination from the RecA-ssDNA/dsDNA structures. *Nature*, **453**, 489–494.
13. Danilowicz,C., Limouse,C., Hatch,K., Conover,A., Coljee,V.W., Kleckner,N. and Prentiss,M. (2009) The structure of DNA overstretched from the 5′ 5′ ends differs from the structure of DNA overstretched from the 3′ 3′ ends. *Proc. Natl Acad. Sci. USA*, **106**, 13196–13201.
14. Danilowicz,C., Hatch,K., Conover,A., Ducas,T., Gunaratne,R., Coljee,V.W. and Prentiss,M. (2010) Study of force induced melting of dsDNA as a function of length and conformation. *J. Phys. Condens. Matter*, **22**, 414106.
15. Smith,S.B., Cui,Y. and Bustamante,C. (1996) Overstretching B-DNA: the elastic response of individual double-stranded and single stranded DNA molecules. *Science*, **271**, 795–799.
16. Danilowicz,C., Coljee,V.W., Bouzigues,C., Lubensky,D.K., Nelson,D.R. and Prentiss,M. (2003) DNA unzipped under a constant force exhibits multiple metastable intermediates. *Proc. Natl Acad. Sci. USA*, **100**, 1694–1699.
17. Rould,E., Muniyappa,K. and Radding,C.M. (1992) Unwinding of heterologous DNA by RecA protein during the search for homologous sequences. *J. Mol. Biol.*, **226**, 127–139.
18. Bazemore,L.R., Folta-Stogniew,E., Takahashi,M. and Radding,C.M. (1997) RecA tests homology at both pairing and strand exchange. *Proc. Natl Acad. Sci. USA*, **94**, 11863–11868.
19. Menetski,J.P., Bear,D.G. and Kowalczykowski,S.C. (1990) Stable DNA heteroduplex formation catalyzed by the Escherichia coli RecA protein in the absence of ATP hydrolysis. *Proc. Natl Acad. Sci. USA*, **87**, 21–25.
20. Saenger,W. (1983) Principles of Nucleic Acid Structure, Springer Advanced Text in Chemistry. Springer, New York, NY.
21. Menetski,J.P., Varghese,A. and Kowalczykowski,S.C. (1988) Properties of the high affinity single-stranded DNA binding state of the Escherichia coli recA protein. *Biochemistry*, **27**, 1205–1212.
22. Zaitsev,E.N. and Kowalczykowski,S.C. (1998) Binding of double-stranded DNA by Escherichia coli RecA protein monitored by a fluorescent dye displacement assay. *Nucleic Acids Res.*, **26**, 650–654.
23. Galletto,R., Amitani,I., Baskin,R.J. and Kowalczykowski,S.C. (2006) Direct observation of individual RecA filaments assembling on single DNA molecules. *Nature*, **443**, 875–878.
24. van der Heijden,T., Van Noort,J., van Leest,H., Kanaar,R., Wyman,C., Dekker,N. and Dekker,C. (2005) Torque-limited RecA polymerization on dsDNA. *Nucleic Acids Res.*, **33**, 2099–2105.
25. Rosselli,W. and Stasiak,A. (1990) Energetics of RecA-mediated recombination reactions: without ATP hydrolysis RecA can mediate polar strand exchange but is unable to recycle. *J. Mol. Biol.*, **216**, 335–352.
26. Shivashankar,G.V., Feingold,M., Krichevsky,O. and Libchaber,A. (1999) RecA polymerization on double-stranded DNA by using single-molecule manipulation: the role of ATP hydrolysis. *Proc. Natl Acad. Sci. USA*, **96**, 7916–7921.
27. Leger,J.F., Robert,J., Bourdieu,L., Chatenay,D. and Marko,J.F. (1998) RecA binding to a single double-stranded DNA molecule: A possible role of DNA conformational fluctuations. *Proc. Natl Acad. Sci. USA*, **95**, 12295–12299.
28. Hegner,M., Smith,S.B. and Bustamante,C. (1999) Polymerization and mechanical properties of single RecA-DNA filaments. *Proc. Natl Acad. Sci. USA*, **96**, 10109–10114.
29. Feinstein,E., Danilowicz,C., Conover,A., Gunaratne,R., Kleckner,N. and Prentiss,M. (2011) Single molecule studies of the stringency factors and rates governing the polymerization of RecA on double stranded DNA. *Nucleic Acids Res.*, **39**, 3781–3791.
30. van Mameren,J., Modesti,M., Kanaar,R., Wyman,C., Peterman,E.J.G. and Wuite,G.J.L. (2009) Counting RAD51 proteins disassembling from nucleoprotein filaments under tension. *Nature*, **457**, 745–748.
31. Essevaz-Roulet,B., Bockelmann,U. and Heslot,F. (1997) Mechanical separation of the complementary strands of DNA. *Proc. Natl Acad. Sci. USA*, **94**, 11935–11940.
32. Hatch,K., Danilowicz,C., Coljee,V. and Prentiss,M. (2007) Measurements of the hysteresis in unzipping and rezipping double-stranded DNA. *Phys. Rev. E*, **75**, 051908.
33. Mazin,A.V. and Kowalczykowski,S.C. (1998) The function of the secondary DNA-binding site of RecA protein during DNA strand exchange. *EMBO J.*, **17**, 1161–1168.
34. van der Heijden,T., Modesti,M., Hage,S., Kanaar,R., Wyman,C. and Dekker,C. (2008) Homologous recombination in real time: DNA strand exchange by RecA. *Mol. Cell*, **30**, 530–538.
35. Bertucat,G., Lavery,R. and Prévost,C. (1999) A molecular model for RecA-promoted strand exchange via parallel triple-stranded helices *Biophys. J.*, **77**, 1562–1576.
36. Kosikov,K.M., Gorin,A.A., Zhurkin,V.B. and Olson,W.K. (1999) DNA stretching and compression: large-scale simulations of double helical structures. *J. Mol. Biol.*, **289**, 1301–1326.